Reactive uptake coefficients for N_2O_5 determined from aircraft measurements during the Second Texas Air Quality Study: Comparison to current model parameterizations

Steven S. Brown, ^{1,2} William P. Dubé, ^{1,2} Hendrik Fuchs, ^{1,2,3} Thomas B. Ryerson, ¹ Adam G. Wollny, ^{1,2,4} Charles A. Brock, ¹ Roya Bahreini, ^{1,2} Ann M. Middlebrook, ¹ J. Andrew Neuman, ^{1,2} Elliot Atlas, ⁵ James M. Roberts, ¹ Hans D. Osthoff, ^{1,2,6} Michael Trainer, ¹ Frederick C. Fehsenfeld, ^{1,2} and A. R. Ravishankara^{1,7}

Received 31 December 2008; revised 26 March 2009; accepted 1 April 2009; published 6 June 2009.

[1] This paper presents determinations of reactive uptake coefficients for N_2O_5 , $\gamma(N_2O_5)$, on aerosols from nighttime aircraft measurements of ozone, nitrogen oxides, and aerosol surface area on the NOAA P-3 during Second Texas Air Quality Study (TexAQS II). Determinations based on both the steady state approximation for NO_3 and N_2O_5 and a plume modeling approach yielded $\gamma(N_2O_5)$ substantially smaller than current parameterizations used for atmospheric modeling and generally in the range $0.5-6\times 10^{-3}$. Dependence of $\gamma(N_2O_5)$ on variables such as relative humidity and aerosol composition was not apparent in the determinations, although there was considerable scatter in the data. Determinations were also inconsistent with current parameterizations of the rate coefficient for homogenous hydrolysis of N_2O_5 by water vapor, which may be as much as a factor of 10 too large. Nocturnal halogen activation via conversion of N_2O_5 to $CINO_2$ on chloride aerosol was not determinable from these data, although limits based on laboratory parameterizations and maximum nonrefractory aerosol chloride content showed that this chemistry could have been comparable to direct production of HNO_3 in some cases.

Citation: Brown, S. S., et al. (2009), Reactive uptake coefficients for N_2O_5 determined from aircraft measurements during the Second Texas Air Quality Study: Comparison to current model parameterizations, *J. Geophys. Res.*, 114, D00F10, doi:10.1029/2008JD011679.

1. Introduction

[2] Hydrolysis of N_2O_5 is one of the most important reactions determining the atmospheric lifetime of NO_x against its conversion to soluble nitrate (NO_3^-) [Dentener and Crutzen, 1993; Tie et al., 2003]. The reaction occurs principally in the dark because of the photochemical instability of the nitrate radical, NO_3 , the precursor to N_2O_5 . It provides a nonphotochemical route for conversion of NO_x to soluble nitrate that is competitive with photochemical reaction of OH with NO_2 [Jones and Seinfeld, 1983]. The hydrolysis reaction occurs rapidly by heterogeneous uptake

[3] Global and regional atmospheric chemistry models rely on parameterizations of the heterogeneous uptake coefficient, $\gamma(N_2O_5)$, that are based on laboratory measurements Until recently, tropospheric models had typically used a large, constant value of $\gamma(N_2O_5)=0.1$, independent of temperature, relative humidity or aerosol composition [Dentener and Crutzen, 1993; Tie et al., 2003]. More recent parameterizations have taken these variables into account on the basis of the availability of more detailed laboratory studies. Evans and Jacob [2005] developed a parameterization that incorporated relative humidity and temperature dependences of $\gamma(N_2O_5)$ on various aerosol types, including

Copyright 2009 by the American Geophysical Union. 0148-0227/09/2008JD011679

D00F10 1 of 16

to aerosol [Mozurkewich and Calvert, 1988] but may also occur more slowly in the gas phase [Wahner et al., 1998a]. Accurate characterization of the rate of N₂O₅ hydrolysis is important to predictions of global tropospheric oxidant burdens [Bell et al., 2005; Evans and Jacob, 2005; Lamarque et al., 2005; Tie et al., 2001] and radiative forcing due to ozone and aerosol [Feng and Penner, 2007; Liao and Seinfeld, 2005]. Hydrolysis of N₂O₅ affects regional air quality through its roles in regulating the reactive nitrogen budget and photochemical ozone production [Riemer et al., 2003], spatial patterns of acid deposition [Calvert et al., 1985] and nitrate aerosol formation [Mathur et al., 2008; Schaap et al., 2004].

¹Earth System Research Laboratory, NOAA, Boulder, Colorado, USA. ²Cooperative Institute for Research in Environmental Sciences, University of Colorado, Boulder, Colorado, USA.

³Now at ICG-2, Forschungszentrum Jülich GmbH, Jülich, Germany.

⁴Now at Max Planck Institute for Chemistry, Mainz, Germany.

⁵Marine and Atmospheric Chemistry, RSMAS, University of Miami, Miami, Florida, USA.

⁶Now at Department of Chemistry, University of Calgary, Calgary, Alberta, Canada.

⁷Department of Chemistry and Biochemistry, University of Colorado, Boulder, Colorado, USA.

sulfate, organic carbon, black carbon, sea salt and dust for use in the GEOS-CHEM model. Davis et al. [2008] incorporated relative humidity and temperature dependences of $\gamma(N_2O_5)$ for a variety of inorganic aerosol types, including ammonium sulfate, bisulfate and nitrate, although omitting organic aerosol. The parameterization was intended for use in regional air quality models. Additional studies have examined specific effects of different aerosol types to demonstrate the implications of particular laboratory studies or to examine these effects in the context of regional models. Several studies have examined the suppression of $\gamma(N_2O_5)$ on nitrate aerosol (the so-called "nitrate effect") [Hallquist et al., 2003; Mentel et al., 1999; Wahner et al., 1998b]. Both Wahner et al. [1998b] and Riemer et al. [2003] parameterized this effect, with the latter applied to regional studies of NO_x, O₃ and aerosol. Organic coatings are known to lead to suppression of $\gamma(N_2O_5)$, and formalisms have been developed to describe this reduction due to condensation of organic aerosol on inorganic cores [Anttila et al., 2006]. In addition to the heterogeneous hydrolysis, laboratory studies have examined the direct gas phase reaction of N₂O₅ with water vapor [Hjorth et al., 1987; Mentel et al., 1996; Tuazon et al., 1983; Wahner et al., 1998a], which can substantially increase the rate of N₂O₅ hydrolysis compared to heterogeneous uptake alone [e.g., Ambrose et al., 2007]. Homogeneous N₂O₅ hydrolysis is part of the IUPAC recommendation for atmospheric modeling and is thus a standard input to models such as the Master Chemical Mechanism [Atkinson et al., 2004].

[4] There are few studies that have directly tested the validity of parameterizations for heterogeneous N₂O₅ uptake coefficients, the rate coefficients for the homogeneous reaction, or the underlying laboratory data, based on atmospheric observations of N₂O₅. Surface level measurements of NO₃ by differential optical absorption spectroscopy (DOAS) and of NO₃ and N₂O₅ by in situ methods have generally shown evidence for rapid N₂O₅ hydrolysis [e.g., Aldener et al., 2006; Allan et al., 1999; Ambrose et al., 2007; Apodaca et al., 2008; Ayers and Simpson, 2006; Brown et al., 2004; Geyer et al., 2001; Heintz et al., 1996; Martinez et al., 2000; Platt et al., 1984; Smith et al., 1995; Vrekoussis et al., 2007; Wood et al., 2005]. Similar observations at higher elevation sites within the free troposphere or from vertical profiling by remote sensing have generally shown longer NO₃ lifetimes, perhaps indicating a lesser role for N₂O₅ hydrolysis [e.g., Allan et al., 2002; Carslaw et al., 1997; von Friedeburg et al., 2002]. Recent aircraft measurements in the Northeast U.S. have shown evidence for large variability in $\gamma(N_2O_5)$ and have used in situ measurements of NO₃ and N₂O₅ to derive quantitative heterogeneous uptake coefficients for direct comparison to model parameterizations [Brown et al., 2006a, 2006b]. However, the aircraft database is limited to only a single regional study and has to date demonstrated only the role of sulfate aerosol in promoting rapid N₂O₅ hydrolysis, with small values for other aerosol types. Recent direct measurements of N2O5 reactivity using a flow tube apparatus and aerosol sampled directly from ambient air have shown $\gamma(N_2O_5)$ smaller than parameterizations, with a positive dependence on both relative humidity and aerosol sulfate content (T. H. Bertram et al., Direct observations of N₂O₅ reactivity: Insights on particulate water content and

implications for NO_x processing rates, submitted to Geophysical Research Letters, 2009).

[5] This paper presents nighttime aircraft measurements from the NOAA P-3 from the 2006 Second Texas Air Quality Study (TexAQS II) [Parrish et al., 2009]. Similar to the previous aircraft study from the northeast United States, analysis of observed NO₃ and N₂O₅ in terms of a steady state between their production and loss provided a determination of heterogeneous N₂O₅ uptake coefficients. Further comparison of the data to model simulations of HNO₃ production corroborate the steady state analysis. The field determinations for $\gamma(N_2O_5)$ are compared to parameterizations for the uptake coefficients, and overall lifetimes of N₂O₅ are compared to tabulated rate coefficients for homogeneous hydrolysis. In general, the results show smaller uptake coefficients and longer N₂O₅ lifetimes than the tabulation and indicate the potential for errors in the representation of nighttime nitrogen oxide chemistry in current models.

2. Field Measurements and Nighttime Aircraft Data

[6] There were four night flights during TexAQS II, three of which flew late enough into the night to be suitable for determination of $\gamma(N_2O_5)$ by the steady state analysis (section 3). Table 1 lists the trace gas and aerosol measurements relevant to this analysis. The instrument for measurement of NO₃ and N₂O₅ was a four-channel cavity ringdown spectrometer that detects NO₃ by 662-nm optical extinction in an ambient temperature channel and the sum of NO₃ and N₂O₅ in a second 662-nm channel with a heated inlet to convert N₂O₅ to NO₃ [Dubé et al., 2006]. Inlet transmission efficiencies were calibrated via reaction of NO₃ with NO to give NO₂, which was measured in two additional 532-nm cavity ring-down channel according to the method of Fuchs et al. [2008]. Figures 1 and 2 show flight tracks and data for the night flights of 8 and 12 October 2006, the two flights on which the majority of $\gamma(N_2O_5)$ determinations were obtained. The flight tracks are color and size coded according to NO3 and numbered according to the NO_x plumes analyzed to determine $\gamma(N_2O_5)$. Time series in Figures 1 and 2 show the data for O₃, NO₂, NO₃, N₂O₅ and aircraft altitude plotted against the time since sunset.

3. Determination of $\gamma(N_2O_5)$ From Steady State Analysis

[7] Steady state lifetimes for NO_3 and N_2O_5 are a standard analysis tool used to assess the reactivity of these compounds [*Platt et al.*, 1984]. The assumption of steady state regards NO_3 and N_2O_5 as reactive intermediates produced from the oxidation of NO_2 by O_3 and lost via. oxidation (NO_3) or hydrolysis (N_2O_5) reactions.

$$NO_2 + O_3 \rightarrow NO_3 + O_2 k_1,$$
 (1)

$$NO_3 + NO_2 \leftrightharpoons N_2O_5 K_{eq},$$
 (2)

Table 1. Instruments Used for Analysis of N₂O₅ Uptake Coefficients

Measurement/Technique	Accuracy	Frequency	Reference	
NO ₃ , N ₂ O ₅ /CRDS ^a	20%	1 Hz	Dubé et al. [2006]	
NO, NO ₂ , O ₃ /	3-8%	1 Hz	Ryerson et al. [1999, 2000]	
chemiluminescence				
HNO ₃ /CIMS ^b	15%	1 Hz	Neuman et al. [2002]	
Aerosol surface area density/ particle counters ^c	25%	1 Hz	Brock et al. [2003], Wilson et al. [2004]	
Aerosol composition/AMS ^d	30%	0.1 Hz	Bahreini et al. [2003, also submitted manuscript, 2009]	
Speciated VOC/can samples ^e	5-10%	80/flight	Schauffler et al. [1999]	

^aCavity ring-down spectroscopy.

$$NO_3 + VOC \rightarrow Products k_{NO_3},$$
 (3)

$$N_2O_5 + H_2O \rightarrow 2HNO_3 \ k_{N_2O_5}.$$
 (4)

Here, k_1 and K_{eq} are the bimolecular rate coefficients and temperature-dependent equilibrium constants for reactions (1) and (2), respectively, and $k_{\rm NO3}$ and $k_{\rm N2O5}$ are the total first-order rate coefficients for loss of NO₃ and N₂O₅ in reactions (3) and (4). Sinks for NO₃ in reaction (3) are represented as VOC oxidation reactions, although the total sink for NO₃ may also include heterogeneous loss to aerosol. Photolysis of NO₃ was unimportant for nighttime aircraft sampling; aside from a few specific instances (not analyzed here), reaction of NO₃ with NO was also generally unimportant. Hydrolysis of N₂O₅ in reaction (4) may include both homogeneous and heterogeneous reactions, as discussed further below. Heterogeneous uptake of N₂O₅ may also lead to additional products, such as ClNO₂, that will be considered explicitly in section 7.

[8] The steady state lifetimes of NO₃, N₂O₅ and their sum (NO₃ + N₂O₅), τ_{NO3} , τ_{N2O5} and τ_{Sum} , are the ratios of the observed concentrations to the NO₃ production rate from reaction (1), P(NO₃) = k₁[O₃][NO₂]. The inverse lifetimes, also referred to as the loss frequencies [*Geyer and Platt*, 2002], can be related to the total first-order sink rate coefficients in reactions (3) and (4), k_{NO3} and k_{N2O5} [*Brown et al.*, 2006b, 2003; *Heintz et al.*, 1996].

$$\tau_{NO_3}^{-1} \equiv \frac{k_1[O_3][NO_2]}{[NO_3]} \approx k_{NO_3} + K_{eq}[NO_2]k_{N_2O_5}, \tag{5}$$

$$\tau_{N_2O_5}^{-1} \equiv \frac{k_1[O_3][NO_2]}{[N_2O_5]} \approx k_{N_2O_5} + \frac{k_{NO_3}}{K_{eq}[NO_2]}, \tag{6}$$

$$\tau_{Sum}^{-1} \equiv \frac{k_1[O_3][NO_2]}{[NO_3] + [N_2O_5]} \approx \frac{k_{NO_3} + K_{eq}[NO_2]k_{N_2O_5}}{1 + K_{eq}[NO_2]}.$$
 (7)

Here the approximate equalities indicate the steady state approximation (see below). The linear relationships between τ_{NO3}^{-1} and $K_{eq}[NO_2]$ in equation (5) and $\tau_{\rm N2O5}^{-1}$ and $1/K_{\rm eq}[{\rm NO_2}]$ in equation (6) allow for individual determination of the two sink rate coefficients as the slopes and intercepts of the inverse lifetimes as a function of the unitless weighting factor, K_{eq}[NO₂], which is equal to the ratio of N₂O₅ to NO₃ at equilibrium. The relationship between this weighting factor and τ_{SUM} in equation (7) is not linear but can be similarly fit to determine k_{NO3} and k_{N2O5}. All three equations contain identical information so that they can be used in combination for consistency, or separately if, for example, one of the instrument channels produced higher quality or more reliable data than another (not generally the case for the measurements described here).

[9] Nighttime aircraft transects of NO₂-containing pollution plumes within the residual daytime boundary layer (i.e., below the mixing height from the preceding day, but above the nocturnal boundary layer) provide data that are well-suited to this analysis. The plume transects sample a range in NO₂ and therefore in the weighting factor, $K_{eq}[NO_2]$, allowing for robust fits to equations (5)–(7). In contrast to surface sampling, aircraft transects also provide nearly instantaneous (several minutes at most) snapshots of individual plumes that are not influenced by chemical evolution within the duration of the measurement. Finally, plumes within the residual layer at night are commonly decoupled from surface level emissions and are therefore more likely to have had sufficient time to achieve steady state in the absence of recent NO_x input.

[10] Determination of the individual sink rate coefficient for N_2O_5 provides a measurement of the uptake coefficient, $\gamma(N_2O_5)$ if the aerosol surface area density (S_A) is known (see Table 1) and if N_2O_5 hydrolysis occurs exclusively by heterogeneous uptake to aerosol rather than in the gas phase.

$$k_{N_2O_5} = \frac{1}{4} \overline{c} \gamma(N_2O_5) S_A$$
 (8)

^bChemical ionization mass spectrometry.

^cMeasurements at 7% RH were corrected to ambient conditions using a parameterization for hygroscopic growth based on the measured change in extinction between dry and ambient relative humidity using a cavity ring-down aerosol extinction spectrometer [Baynard et al., 2007]. The surface area correction factor, $SA_{correction}$, was $SA_{Correction} = (1 + 5.9672 \times 10^{-6} RH^{2.0868} + 3.4005 \times 10^{-5} RH^{2.1255})^2$. For RH < 75% the correction factors for surface area were <1.8, and the combined uncertainty of the measurement and the growth correction was 25% based on the deviation of Mie scattering calculations with observed RH dependence of aerosol extinction. Above 75% RH the uncertainties due to the hygroscopic growth became substantially larger.

^dCompact time of flight aerosol mass spectrometer.

^eAnalyzed by GC-MS.

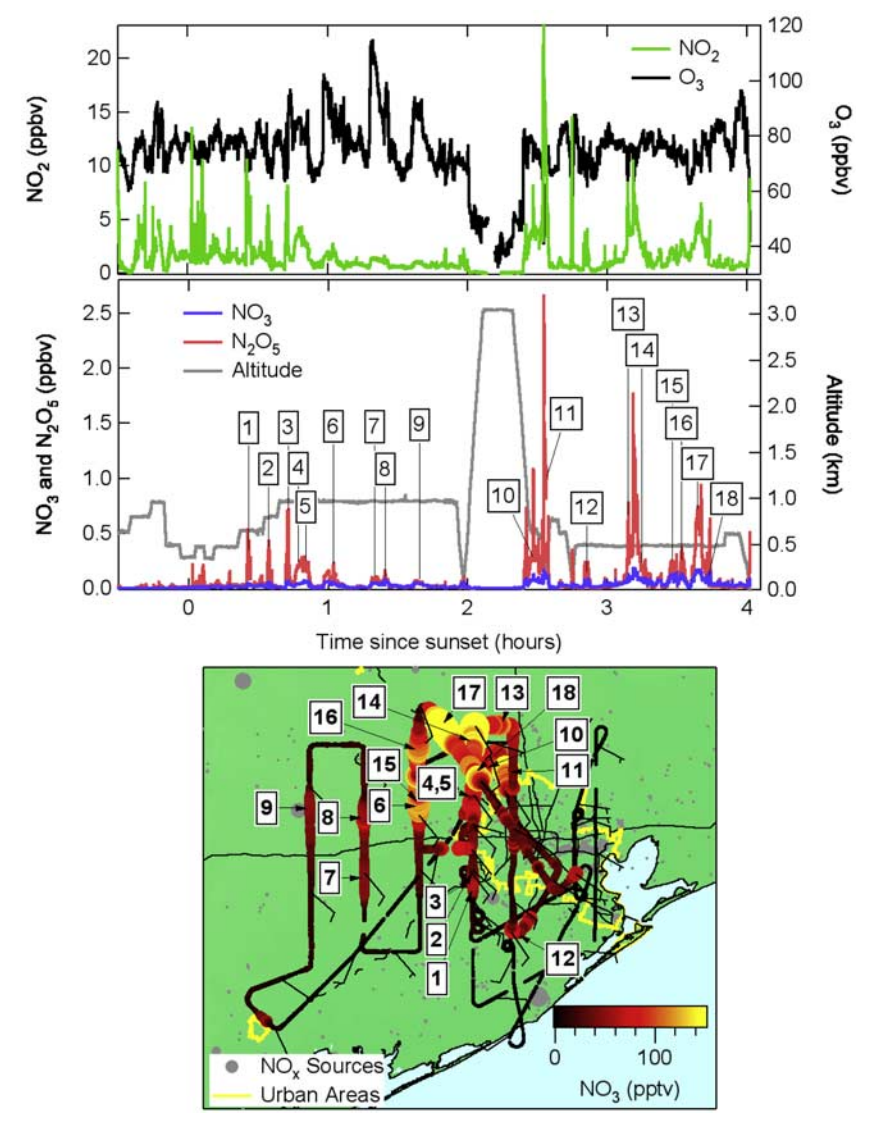


Figure 1. (top) Mixing ratios of O_3 , NO_2 , NO_3 , N_2O_5 , and aircraft altitude plotted as a function of time since sunset (defined as solar zenith angle of 90°) for the 8 October 2006 flight. (bottom) Map of the Houston area (urban boundary outlined in yellow) with the P-3 flight track superimposed. The flight track is color- and size-coded by NO_3 mixing ratio. The numbers in the top and bottom plots are the individual NO_x plumes analyzed to determine $\gamma(N_2O_5)$ values.

Here, \overline{c} is the mean molecular speed of N_2O_5 from gas kinetic theory. Equation (8) is valid for submicron aerosol, which constituted the majority (>96%) of the aerosol surface area during the TexAQS campaign, and for small uptake coefficients (<0.1) such that gas phase diffusion to the particle surface does not limit the uptake rate [Fuchs and Stugnin, 1970]. There are two principal uncertainties in this method for determining $\gamma(N_2O_5)$. The first is the time required for the approach to steady state, as described in more detail below. The second is potential covariance between the independent variable, K_{eq}[NO₂] in equations (5)–(7), and the sink rate coefficients, k_{NO3} and k_{N2O5} . These covariances arise from correlation between NO2 and either reactive VOC (influencing k_{NO3}) or aerosol surface area (influencing k_{N2O5}). The latter is a particular concern for determinations of $\gamma(N_2O_5)$ in this study since aerosol surface area was frequently correlated with NO2 in nighttime plumes sampled during TexAQS II. Substitution of equation (8) into equations (5)–(7) yields a different set of equations that accounts for this covariance.

$$\tau_{NO_3}^{-1} \approx k_{NO_3} + \frac{1}{4} \overline{c} S_A K_{eq} [NO_2] \gamma (N_2 O_5)$$
 (9)

$$\tau_{N_2O_5}^{-1}K_{eq}[NO_2] \approx k_{NO_3} + \frac{1}{4}\overline{c}S_AK_{eq}[NO_2]\gamma(N_2O_5) \eqno(10)$$

$$\tau_{Sum}^{-1} \left(1 + K_{eq}[NO_2] \right) \approx k_{NO_3} + \frac{1}{4} \overline{c} S_A K_{eq}[NO_2] \gamma(N_2 O_5) \quad (11)$$

The independent variable in equations (9)–(11) is $\overline{c}S_AK_{eq}[NO_2]/4$, and the quantities on the left-hand sides

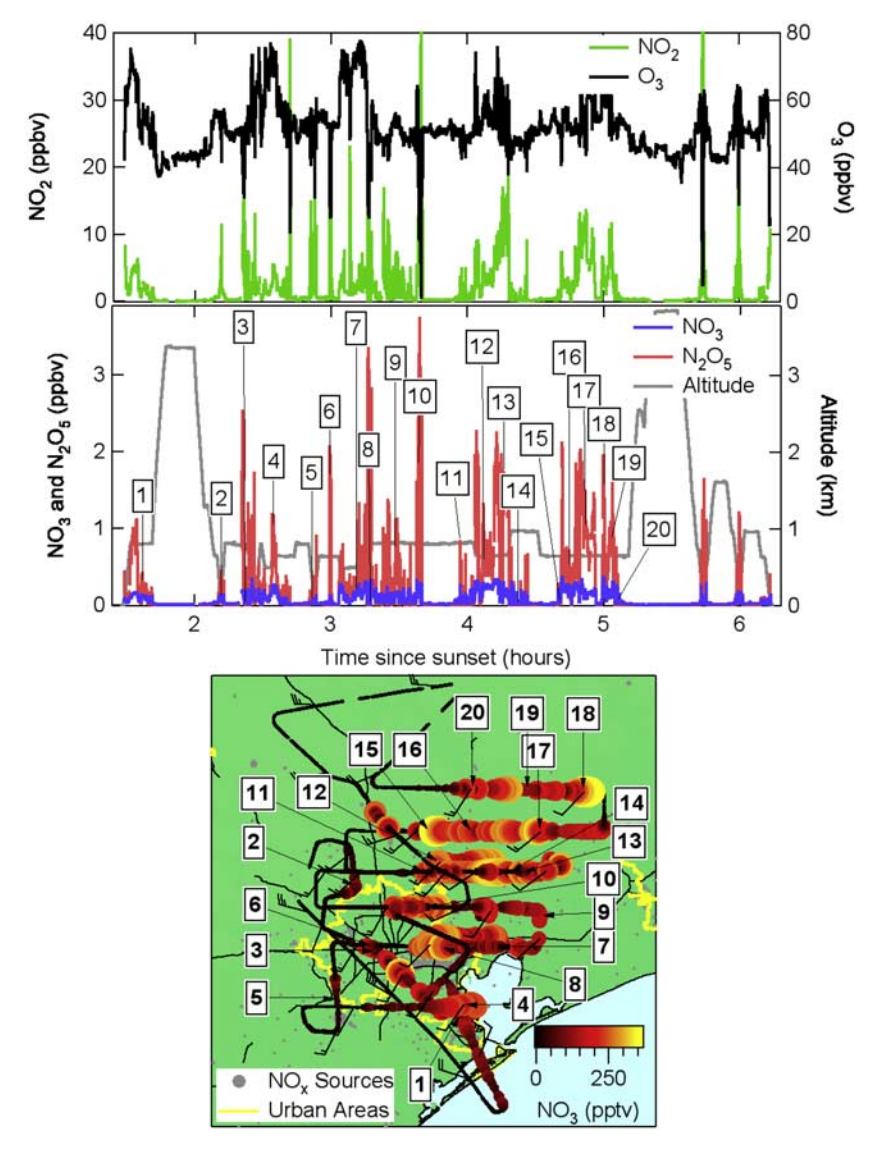


Figure 2. Same as Figure 1 but for the 12 October 2006 flight.

have been multiplied by the appropriate weighting factor to make the right-hand sides identical. Fits to equations (9)–(11) not only account for covariance between NO₂ and S_A , but also yield γ (N₂O₅) directly as the slope of a linear fit.

[11] Figures 3 and 4 shows example data and fits for single plumes from the 8 and 12 October 2006 flights. The plume in Figure 3 was sampled to the northwest of Houston, 3.7 h after local sunset on 8 October (plume 18 in Figure 1). A calculated backward trajectory (R. R. Draxler and G. D. Rolph, HYSPLIT (HYbrid Single-Particle Lagrangian Integrated Tracker) Model, 2003, http://www.arl.noaa.gov/ ready/hysplit4.html) placed the air mass near the Houston ship channel 4-5 h prior to sampling. Figure 3 shows plots of the steady state lifetimes according to equations (9)–(11)and the best fit values of $\gamma(N_2O_5)$ and k_{NO3} (listed on Figure 3) as an inverse). The lower left-hand graph shows the time series for the observed NO₃ and N₂O₅ in the plume and the calculated NO₃ and N₂O₅ from the average values of the parameters from the top graphs. As the lower right graph shows, there was a significant correlation between the aerosol surface area and K_{eq}[NO₂], such that fits to

equations (9)–(11) were superior to fits to equations (5)–(7) for determination of $\gamma(N_2O_5)$. The steady state $\gamma(N_2O_5)$ was 0.0028. The relative humidity was 67%, and the aerosol composition was 54% organic (by mass), with the inorganic component fully neutralized as ammonium sulfate and ammonium nitrate. Similar aerosol types gave small $\gamma(N_2O_5)$ values in our previous study in the northeast United States [*Brown et al.*, 2006b]. In spite of the small $\gamma(N_2O_5)$, there was sufficient aerosol surface area in this plume to limit the N_2O_5 lifetime to roughly 2 h, still allowing for significant production of HNO₃ (see below).

[12] Figure 4 shows a similar set of example plots from the 12 October flight for a plume sampled to the northeast of Houston (plume 18 in Figure 2) 5 h after sunset. The transport time for industrial NO_x sources in the Houston ship channel to the point of sampling was 6 h. As in the previous example, the parameters derived from these fits reproduced the observed data in the lower left-hand plot, with $\gamma(N_2O_5)$ values in the range 0.0010–0.0013. Correlations between aerosol surface area and $K_{eq}[NO_2]$ were also evident in this plume. The relative humidity on this transect

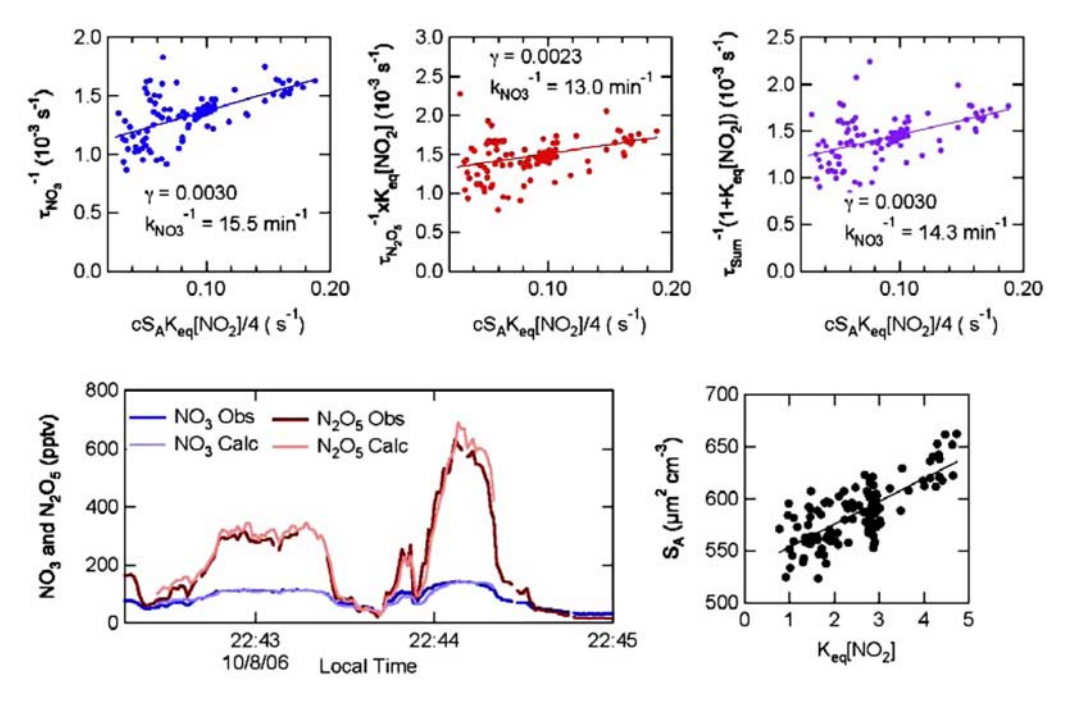


Figure 3. (top) Inverse NO₃ and N₂O₅ steady state lifetimes and of the summed lifetime of NO₃ and N₂O₅ according to equations (9)–(11), for a single NO_x plume intercepted on the 8 October 2006 flight. The text on the plots gives the best fit values of γ (N₂O₅) and k_{NO3} for each fit. (bottom left) Time series of NO₃ and N₂O₅ mixing ratios for this plume and the calculated time series for these data using the average of the fitted parameters from the top plots. (bottom right) Aerosol surface area density against K_{eq}[NO₂] showing the covariance between these quantities (see text).

was 59%, and the submicron aerosol composition was 60% organic with a neutralized ammonium sulfate/ammonium nitrate inorganic fraction. Lifetimes for N_2O_5 were generally longer on the 12 October flight than on 8 October, consistent with the larger measured aerosol surface area and relative humidity on 8 October. There was no significant

difference in average uptake coefficients between the two flights, however.

[13] Table 2 gives all of the $\gamma(N_2O_5)$ values from the three TexAQS II night flights. These determined $\gamma(N_2O_5)$ are mainly from the steady state analysis described above, assuming that all hydrolysis is attributable to heterogeneous

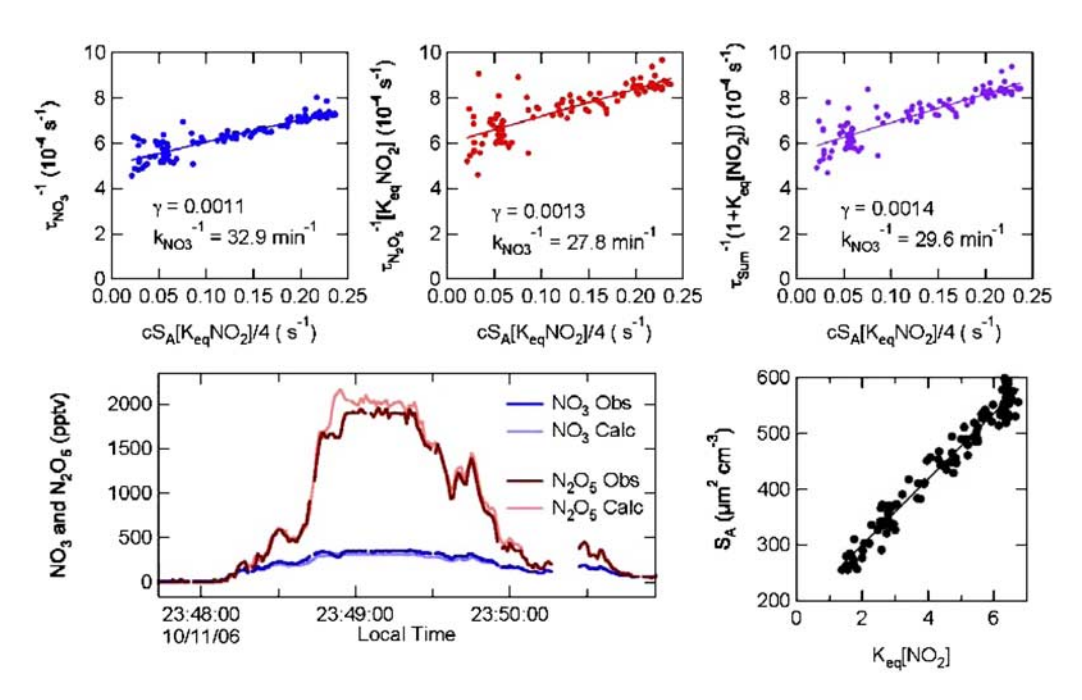


Figure 4. Same as Figure 3 but for a plume intercepted on the 12 October 2006 flight.

Table 2. N₂O₅ Uptake Coefficient Determinations From Three Night Flights

Plume	Organic Mass/Total NO ₃ -/(NO ₃ -					
Number	$\gamma (N_2 O_5)^a$	RH (%)	Mass	$+SO_4^{-2}$)	T (K)	
rumber	/(11/203)			1504	1 (11)	
(0.0050		October	0.12	202.2	
6	0.0059	65	0.59	0.12	292.2	
7	0.0025	67 55	0.53	0.07	292.2	
8	0.0022	55	0.65	0.15	292.5	
9	0.0024	59	0.50	0.06	292.4	
10	0.0030	68	0.59	0.13	294.0	
11	0.0050	67	0.58	0.14	296.4	
14	0.0038	66	0.56	0.11	295.4	
16	0.0009	68	0.55	0.10	295.3	
17	0.0015	68	0.57	0.14	295.2	
18	0.0028	67	0.51	0.06	295.4	
Median	0.0025	67	0.56	0.11	294.0	
$Avg \pm 2\sigma$	0.003 ± 0.002	65 ± 9	0.56 ± 0.08	0.11 ± 0.06	294.1 ± 3.2	
		10 (October			
1	0.0051	85	0.54	0.27	286.7	
2	0.0018	72	0.32	0.09	286.4	
3	0.0036	72	0.39	0.14	285.8	
4	0.0082	65	0.25	0.05	286.9	
5	0.019	72	0.59	0.26	286.5	
Median	0.0051	72	0.39	0.14	286.5	
Avg $\pm 2\sigma$	0.0075 ± 0.014	73 ± 9	0.42 ± 0.28	0.16 ± 0.2	286.5 ± 0.8	
		12 (October			
1	0.0060	41	0.67	0.17	295.0	
3	0.0012^{b}	47	0.58	0.07	294.5	
4	0.0012	62	0.72	0.31	295.1	
6	0.0022^{b}	61	0.55	0.10	295.3	
7	0.0010	64	0.68	0.23	295.3	
8	$0.0020^{\rm b}$	34	0.52	0.07	295.3	
9	0.010	40	0.57	0.09	295.0	
10	0.0006^{b}	48	0.49	0.09	294.4	
12	0.0031	44	0.59	0.13	295.8	
13	0.0053	58	0.57	0.21	295.1	
15	0.0004 ^b	39	0.53	0.08	296.0	
16	0.0062	39	0.59	0.11	296.0	
17	0.0063	56	0.59	0.19	295.1	
18	0.0013	59	0.61	0.14	294.7	
19	0.0055	57	0.57	0.29	295.0	
20	0.0009	39	0.58	0.10	295.8	
Median	0.0020	47	0.58	0.11	295.1	
Avg $\pm 2\sigma$	0.0033 ± 0.0056	49 ± 20	0.59 ± 0.12	0.15 ± 0.15	295.2 ± 1.0	

^aUncertainty estimated at $\pm 45\%$ ($\pm 20\%$ from NO₃, N₂O₅ measurements, $\pm 25\%$ from aerosol surface area measurements, and $\pm 30\%$ from steady state approximation). Uncertainty estimate does not include covariance between NO₂ and VOC, which can skew slopes of steady state analysis plots and lead to larger uncertainty for individual determinations.

uptake, with no correction for homogeneous reaction. Inclusion of homogeneous hydrolysis would further reduce the determined values, but, as section 6 argues, the observed N_2O_5 lifetimes are not consistent with the current parameterization for the homogeneous reaction. Some of the $\gamma(N_2O_5)$ in Table 2 are from plume modeling, rather than the steady state analysis, as described in section 4.

3.1. NO₃ Loss Rate Coefficients

[14] In addition to determining the N_2O_5 reactive uptake coefficients, the steady state analysis determines first-order loss rate coefficients for NO_3 from the intercepts of plots such as those shown in Figures 3 and 4. Comparison of the determined k_{NO3} to that predicted from VOC measurements provides a consistency check on the determination of the

uptake coefficients. Figure 5 shows a plot of the time series of the $k_{\rm NO3}$ from the steady state determinations and those from speciated VOC measurements from canister samples taken periodically on the 8 and 12 October flights. The $k_{\rm NO3}$ from the VOC measurements are the sum of the products of the measured VOC concentrations and the rate coefficient for the corresponding NO₃-VOC reactions [Atkinson and Arey, 2003].

$$k_{NO_3}^{Canister} = \sum_i k_{NO_3 + VOC_i}[VOC_i]. \tag{12}$$

The sum includes all VOCs measured from the canister samples for which NO₃ rate coefficient data are available,

^bDetermined from plume modeling rather than steady state analysis (see text). Uncertainty in this approach estimated at $\pm 35\%$ ($\pm 15\%$ from the HNO₃ measurement, $\pm 25\%$ from the aerosol surface area measurements, and $\pm 20\%$ for plume age determinations).

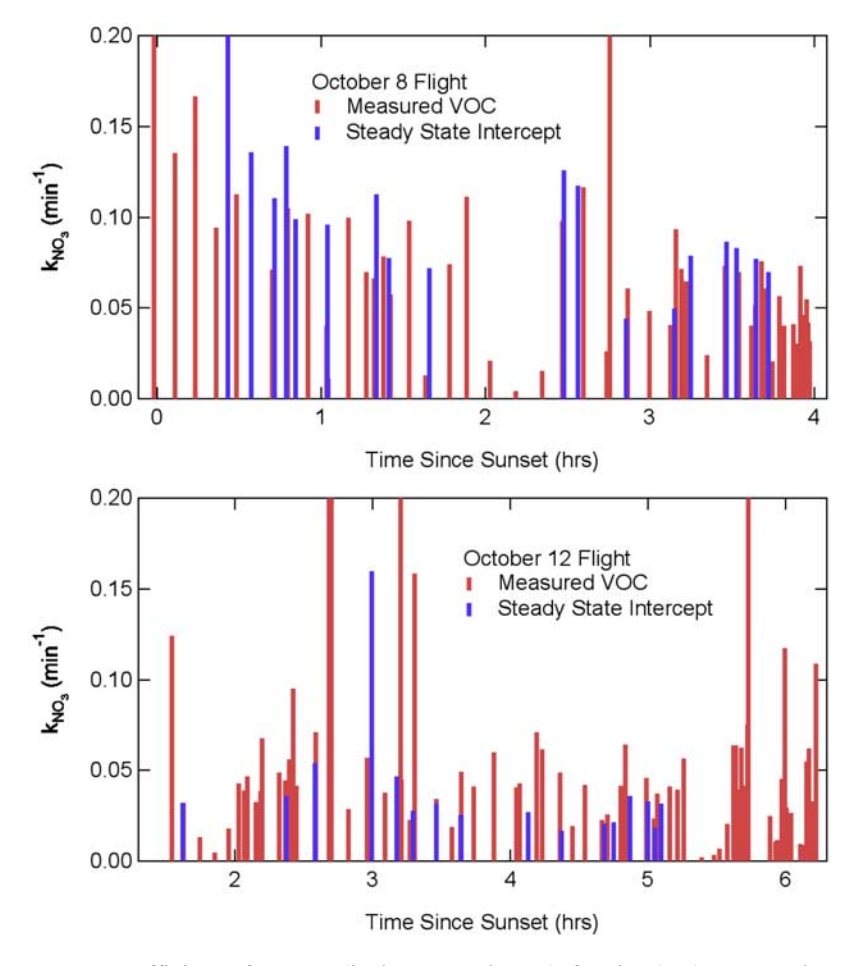


Figure 5. Loss rate coefficients for NO_3 (in inverse minutes) for the (top) 12 October and (bottom) 8 October flights. Red bars show determinations from VOC measurements according to equation (12), and blue bars show determinations from intercepts of the steady state fits in equations (9)–(11).

with the exception of furans, which were measured in some samples but would lead to NO₃ loss rates approximately 1 order of magnitude larger than those seen here. The origin of these compounds in the can samples is not clear. In general, the steady state determinations were not coincident in time with the canister samples, so a direct plume by plume comparison is not possible. However, as the overlay of the two time series shows, the steady state determinations of k_{NO3} were similar to those derived from speciated VOC measurements. For the 8 and 12 October flights, the steady state k_{NO3} were on average 30% larger and 40% smaller, respectively, than those from the canisters. This level of agreement, while not necessarily quantitative owing to sampling limitations, corroborates the $\gamma(N_2O_5)$ determinations by confirming the partitioning of losses between NO₃ and N₂O₅ to within the anticipated 30% uncertainty (see below) of the steady state analysis.

3.2. Validity of Steady State Approximation

[15] One of the chief uncertainties in the determination of $\gamma(N_2O_5)$ from the steady state analysis is the validity of the steady state approximation itself, which requires balance between production in reaction (1) and losses due to reactions (3) and (4). There are three conditions under which this approximation fails. The first is small values for the sink rate coefficients, k_{NO3} and k_{N2O5} , such that a

long induction period (approximately 5 times the inverse of the first-order loss rate coefficient [Pilling and Seakins, 1995]) prevents the system from achieving a steady state [Allan et al., 2000; Carslaw et al., 1997]. The second is the time required to achieve an exact balance between the forward and reverse reactions in (2), (i.e., no slight deviation from equilibrium between NO₂, NO₃ and N₂O₅) at large ratios of N₂O₅ to NO₃ [Brown et al., 2003]. This condition delays the approach to steady state at high NO_x or low temperatures, both of which increase the ratio of N₂O₅ to NO₃. Finally, deviations from steady state may occur if the time scale for mixing is comparable to that of the chemistry itself. This effect is known to be important in nocturnal boundary layers [Stutz et al., 2004], but likely less important within the plumes analyzed here (see below).

[16] Numerical modeling using the four-reaction scheme outlined above (and as described previously [Brown et al., 2003]) provided a check on the time required to achieve steady state for each of the $\gamma(N_2O_5)$ determinations in Table 2. Figure 6 shows two examples from the 8 and 10 October flights. The solid lines are the inverse of the quantity in the center of equations (5) and (6), i.e., the ratio of the concentration of NO_3 and N_2O_5 , respectively, to the NO_3 production rate. The dashed lines are the inverse of the right-hand sides of equations (5) and (6), i.e., (k_{NO3})

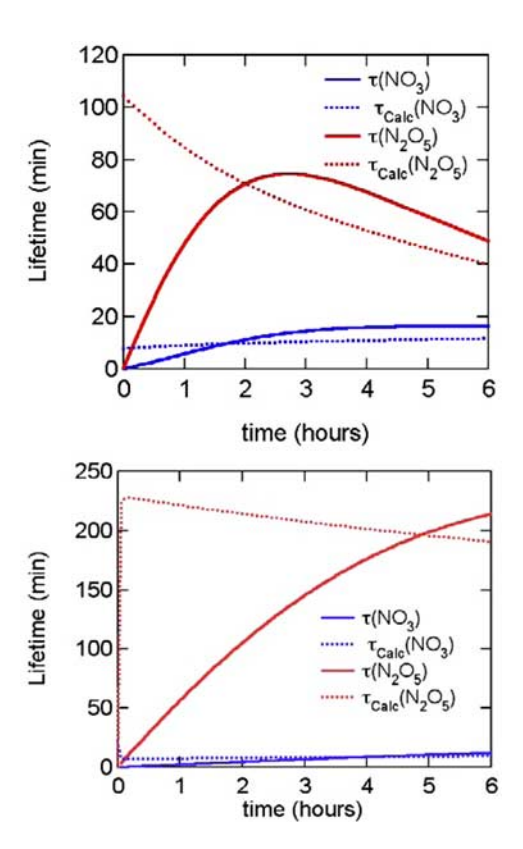


Figure 6. Calculation of approach to steady state for two of the analyzed plumes: (top) mixed urban from 8 October and (bottom) Parish power plant from 12 October. Solid lines are NO_3 and N_2O_5 lifetimes defined in equations (5)–(6), i.e., $\tau(NO_3) = [NO_3]/P(NO_3)$ and $\tau(N_2O_5) = [N_2O_5]/P(NO_3)$. Dashed lines are the sum of the first-order loss rate coefficients according to the right-hand sides of equations (5) and (6). Steady state was achieved (i.e., approximate agreement between the two curves) to within 30% after 2 h in the first example, but required at least 5 h in the second.

 $K_{\rm eq}[NO_2]k_{\rm N2O5})^{-1}$ for the NO_3 plot, and $(k_{\rm N2O5}+k_{\rm NO3}/(K_{\rm eq}[NO_2]))^{-1}$ for the N_2O_5 plot. When the observed steady state lifetimes in the solid lines approximately match the calculated lifetimes in the dashed lines in Figure 6 (to within $\pm 30\%$), the steady state relationships in the equations are approximately valid to within the error of the measurement derived values. The error in the determined $\gamma(N_2O_5)$ due to the approximate steady states can be estimated as the difference between observed and calculated lifetimes.

[17] The calculations use observed ozone, NO_2 and temperature as inputs. The initial NO_2 at the start of the model is predicted from observed NO_2 according to $[NO_2]_0 = [NO_2]_{obs} \exp(k_1[O_3]\Delta t)$, where Δt is the time from either emission or sunset (depending on the plume) to the time of observation. For plumes with evidence for photochemistry, such as those with positive correlations between HNO_3 or PAN and O_3 , the time is taken as that since sunset. For plumes with negative correlations between reactive nitrogen and ozone, the plume time can be estimated as the transport time from a known source, such as a power plant, or from the slope of a plot of O_3 versus NO_2 , as detailed previously $[Brown\ et\ al.,\ 2006a]$. The model also requires inputs for k_{NO_3} and k_{N2O_5} , the quantities determined from the steady

state analysis. Values for $k_{\rm NO3}$ are calculated from VOC data as described above in equation (12). Where such data are not available for a given plume, values or averages of several values from the nearest canister samples are used. Any missing NO₃ reactivity not captured by the canister measurements would make the estimated time to approach steady state an upper limit. Values for $k_{\rm N2O5}$ are then taken from the steady state determination as a check on the model, i.e., if the determined value is large enough for the steady state analysis to be capable of determining it. For most determinations shown here for which steady state was valid, the $k_{\rm NO3}$ were sufficient to bring the system to steady state even if $k_{\rm N2O5}$ were zero.

[18] Figure 6 (top) is a simulation for the same plume shown in Figure 3 for the 8 October flight. The time to approach steady state was less than 2 h, longer than the estimated 4-h transport time for this plume, such that the determined $\gamma(N_2O_5)$ should be accurate to within $\sim 30\%$ on the basis of the differences between observed and calculated steady state lifetimes in Figure 6 (top). Figure 6 (bottom) is a model for an intercept of the Parish coal-fired power plant (identified by large SO₂ emission and an SO₂ to NO_x ratio consistent with emission inventory data [Frost et al., 2006]), located on the southwest side of Houston, on the 12 October flight. Transport time based on local wind speed and direction was 1.4 h while the time to approach steady state was approximately 5 h. Since steady state was likely invalid in this case, the determined $\gamma(N_2O_5)$ was an upper limit to the actual value. Simulations of many of the power plant plume intercepts from TexAQS II, which tended to have high NO_x and low VOC (and thus small k_{NO3}), showed similarly long times for approach to steady state. However, as described below, determinations of $\gamma(N_2O_5)$ were still possible for these sources on the basis of the known transport time and the observed compositions within the plumes.

4. Determination of $\gamma(N_2O_5)$ From Plume Modeling

[19] The model described above can also be used to determine $\gamma(N_2O_5)$ for point emission sources such as power plants. These determinations do not rely on the steady state approximation but instead on the transport time from the source and the observed O₃, NO₂ and HNO₃ levels within the plumes. The model is the same as that described above, initialized by an injection of NO into an O3 background at time zero. The model includes chemical conversion of NO to NO2, which is rapid compared to further oxidation of NO₂ to NO₃. Dilution and mixing during transport were modeled from observations of the widths of plume intercepts at various times downwind from the point of emission. Uncertainty due to dilution primarily affects the evolution of the plume at short times, when the mixing and dilution appear to be more rapid than at later times on the basis of the observations of similar plume widths at multiple distances downwind from the same source. Rapid initial mixing may result from turbulence present upon emission of a relatively warm plume. This process is not represented in the model, which shows only the chemical titration of O₃ subsequent to an instantaneous injection of NO. The model assumes that HNO₃ produced

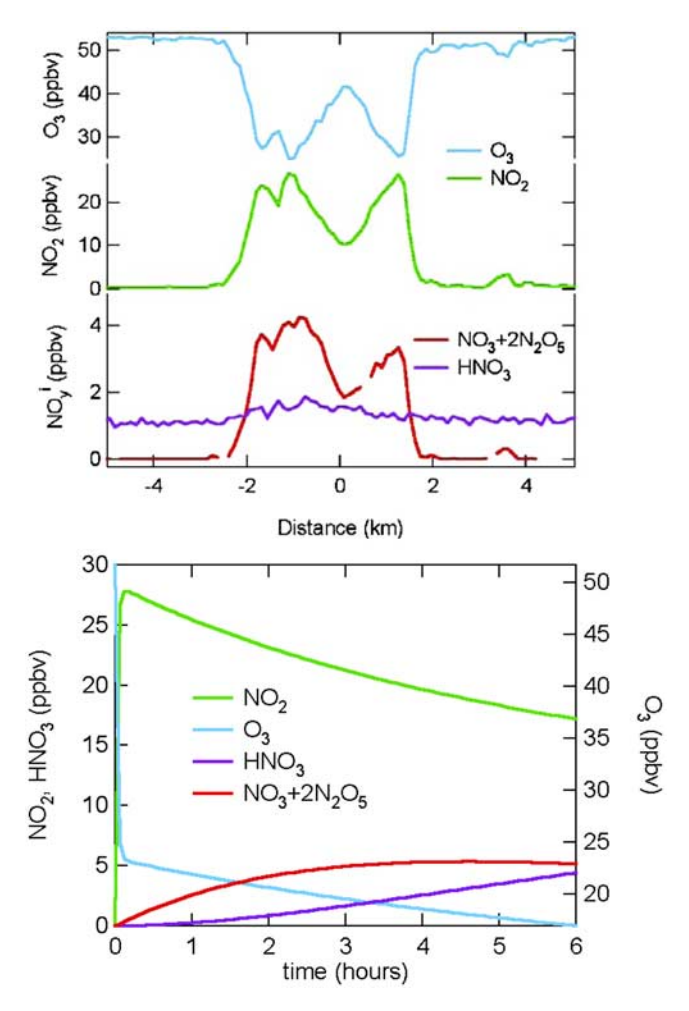


Figure 7. (top) Intercept of a plume from the Parish power plant from the 12 October 2006 flight showing mixing ratios for O_3 , NO_2 , HNO_3 , and the nocturnal nitrogen oxide sum ($NO_3 + 2N_2O_5$), plotted against the distance from plume center. Buildup of HNO_3 was small relative to that of the nocturnal nitrogen oxides. (bottom) Model of the time evolution of nitrogen oxides and ozone at plume center.

from reactions (1)–(4) is conserved in the gas phase during transport and not lost to dry deposition. This assumption is consistent with nighttime plumes that have a finite depth within the residual daytime boundary layer and no contact with the surface [e.g., Brown et al., 2007]. Gas phase HNO₃ was large in comparison to aerosol phase NO_3^- (10-40× for plume analyzed here) such that the latter could be neglected for this analysis. Variation of k_{N2O5} within the model simulations to reproduce the observed HNO₃ enhancements provided a determination for $\gamma(N_2O_5)$ from equation (8) that was independent of the steady state approximation. Figure 7 shows the time series for O₃ and reactive nitrogen (here NO_2 , the sum of $(NO_3 + 2N_2O_5)$ and HNO_3 but not PAN, which was not strongly enhanced) across a plume intercept. This power plant plume is the same for which the steady state analysis was shown to be invalid in Figure 6. Figure 7 (bottom) shows a simulation of the mixing ratios at plume center (taken here as the maximum on one side or the other of the double peaked plume). The observed HNO₃ enhancement of 0.5 ppbv at a transport time of 1.4 h required $k_{\rm N2O5}$ of $5\times 10^{-5}~s^{-1},$ or $\gamma(N_2O_5)=0.002$ at the observed aerosol surface area. The simulation slightly underestimated the observed NO3 and $N_2O_5,$ indicating that the determined transport time based on local wind speed and distance to the source may have been too short for this particular plume (i.e., insufficient time for buildup of these compounds).

[20] Simulation of HNO₃ enhancements within plumes was also useful in corroborating the steady state approximation in cases where it was expected to be approximately correct. The plume shown in Figure 3 from the 8 October flight is one such example. Here, a value of $\gamma(N_2O_5)$ = 0.0016 within the simulation reproduced the observed HNO₃ enhancement of 1.9 ppbv within the plume, shown in Figure 8, for the transport time of 3.7 h since sunset. The $\gamma(N_2O_5)$ from the steady state determination was 70% larger, at 0.0028, but both determinations gave small $\gamma(N_2O_5)$, i.e., substantially below 0.01. The simulation also produces an overall budget for nitrogen transport and/or loss within this plume, shown as the pie chart in Figure 8. At the point of sampling, just over 30% of the NO₂ that had been oxidized during nighttime transport was present as HNO₃, just under 30% as unreacted N₂O₅, and the remainder as the products of NO₃-VOC reactions. Other plumes showed smaller HNO3 enhancements with a greater role for transport of reactive nitrogen as N₂O₅ or loss via NO₃-VOC oxidation. Where possible, the $\gamma(N_2O_5)$ values from the

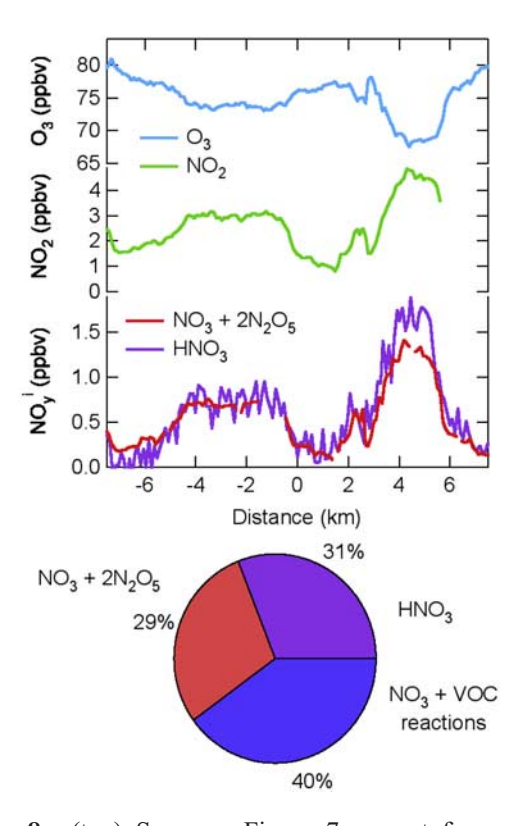


Figure 8. (top) Same as Figure 7, except for a plume intercepted on the 8 October flight. This is the same plume shown in Figure 3. The 3 ppbv background has been subtracted from the HNO₃ data. (bottom) Pie chart showing the modeled contributions of nocturnal nitrogen oxides, HNO₃, and NO₃-VOC reaction products for this plume at the time of intercept.

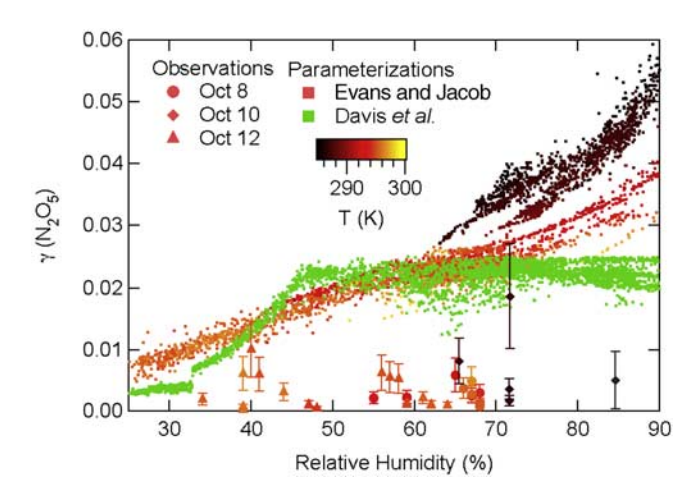


Figure 9. Determined $\gamma(N_2O_5)$ against relative humidity for three night flights, as shown in the legend. Also overlaid is the RH dependence from two recent parameterizations for all of the nighttime data from the three flights. The *Evans and Jacob* [2005] data and the observations are color coded by absolute temperature, as the legend shows.

steady state determinations were corroborated by simulations from observed HNO₃ enhancements.

5. Comparison to Model Parameterizations

[21] The values for $\gamma(N_2O_5)$ determined from these aircraft observations fall generally below 0.01 over a range of relative humidity (RH), temperature and aerosol composition. As such, they are below the range of most laboratory determinations on pure sulfate aerosols but closer to the range determined for some organic aerosol substrates and nitrate salts. They are also generally below the range of most parameterizations that have been published to date for use in atmospheric model studies. Figures 9–12 compare the $\gamma(N_2O_5)$ determined from the three flights during this study to these recent parameterizations as a function of RH, aerosol organic fraction and nitrate to sulfate ratio.

[22] Figure 9 shows the determined $\gamma(N_2O_5)$ against RH for all three flights and two model parameterizations that explicitly consider the dependence of $\gamma(N_2O_5)$ on RH. The points from the model parameterizations are for all nighttime data at the time resolution of the aerosol composition measurements from the AMS (Table 1) and show the variation of $\gamma(N_2O_5)$ with RH for all of the conditions encountered on all three flights. The determinations from individual plumes are fewer in number and more limited in the sampled conditions. The variation in the parameterizations at any given RH is due to the dependence on aerosol composition and temperature. The Evans and Jacob [2005] points show a distinct T dependence, as shown in the color code, while the Davis et al. [2008] points are not strongly T-dependent (no color code). Data for 8 and 12 October clustered between 292 and 296 K, while the more limited data for 10 October was near 286 K, as shown by the color code. Evans and Jacob assumed that organic aerosol have small $\gamma(N_2O_5)$ that is linearly dependent on RH below 57% and a constant, larger value of 0.03 above on the basis of a recent laboratory study [Thornton et al.,

2003] on pure organic substrates. Evans and Jacob [2005] also included elemental carbon, dust and sea salt, though these aspects of their parameterization were not used in this comparison. Davis et al. [2008] did not explicitly consider organic aerosol, instead parameterizing the RH dependence of $\gamma(N_2O_5)$ on inorganic aerosol substrates. Their parameterization considered the RH dependence from several different laboratory studies, but ultimately recommended a dependence that did not include data from Kane et al. [2001], since this study showed a much stronger RH dependence than the others. Davis et al. [2008] also explicitly considered the dependence on aerosol acidity, i.e., between ammonium sulfate ((NH₄)₂SO₄) and bisulfate (NH₄HSO₄). For the TexAQS II data, aerosol composition measurements showed a predominance of ammonium sulfate (and in some cases ammonium nitrate; see below), so the variation in Figures 9-11 does not reflect the acidity dependence of Davis et al. [2008].

[23] In contrast to the two parameterizations, the determined $\gamma(N_2O_5)$ show no clear dependence on RH, and are uniformly low over the studied range of 35-85%. The majority of the data from the 8 October flight cluster in a range between 60 and 70% RH, however, while those from the 12 October flight span a range from 35 to 65%. Levels of RH were higher on the 10 October flight, although there were fewer $\gamma(N_2O_5)$ determinations. There is only a single determination above 73% RH from the entire data set, such that the majority of points do not characterize the high-RH region where Evans and Jacob [2005] show a steep increase in $\gamma(N_2O_5)$. The range of RH represented by the determinations is consistent with that sampled during night flights within the residual daytime boundary layer. RH values within this layer are typically lower than below the nocturnal boundary layer or within the marine boundary layer at night. This effect has been demonstrated in previous vertical profiling studies in the northeast United States [Brown et al., 2007], where observed vertical profiles in RH over small altitude ranges near the surface at night were associ-

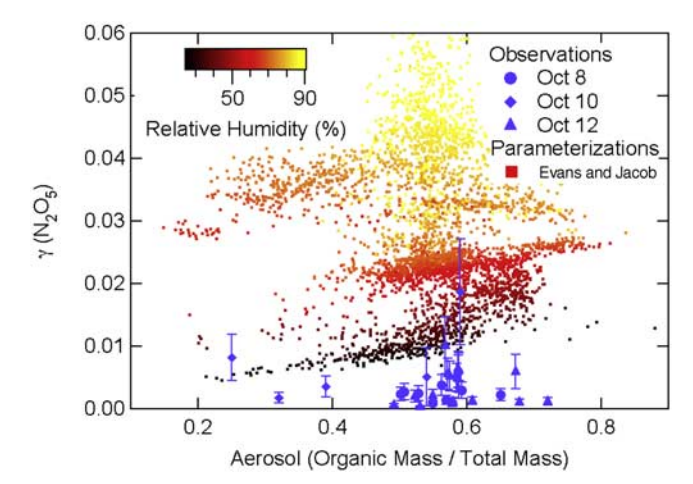


Figure 10. Determined $\gamma(N_2O_5)$ against aerosol organic fraction (from the AMS). The *Evans and Jacob* [2005] parameterization, which has an explicit dependence on organic aerosol, is overlaid and color coded by relative humidity, as shown in the legend.

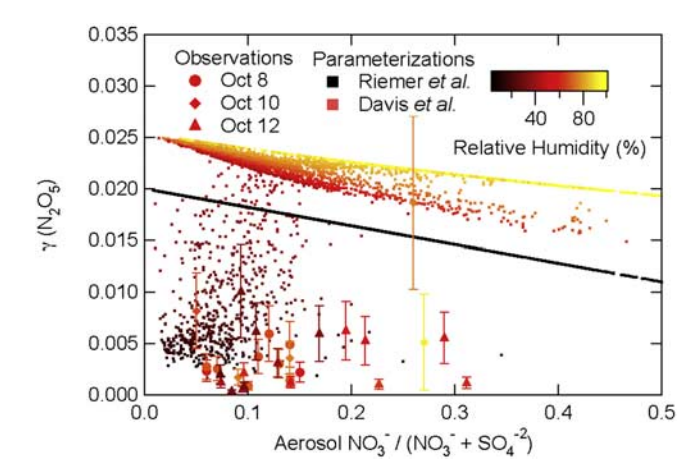


Figure 11. Determined $\gamma(N_2O_5)$ against aerosol nitrate to (nitrate + sulfate) mass ratio (from the AMS) for the three flights. Overlaid is data from the parameterizations that include a nitrate effect (see text). Points for *Davis et al.* [2008] are color coded by relative humidity.

ated with changes in particle surface area and, potentially, N_2O_5 hydrolysis rates.

[24] One potential reason for the lack of agreement between the RH dependences in the determinations and parameterizations is the presence of organic aerosol, which as noted above, is neglected in some parameterizations. Figure 10 shows the variation in determined $\gamma(N_2O_5)$ with aerosol organic fraction (defined here as the organic mass to total aerosol mass ratio from the AMS) along with that for the Evans and Jacob [2005] parameterization. The comparison suggests that if the smaller $\gamma(N_2O_5)$ determined from the field data are the result of organic aerosol, then the parameterization does not fully characterize the magnitude of the reduction. A variety of laboratory studies have suggested reductions in $\gamma(N_2O_5)$ due to organic aerosol similar to those seen in the field determinations [Badger et al., 2006; Cosman and Bertram, 2008; Cosman et al., 2008; Folkers et al., 2003; McNeill et al., 2006; Park et al., 2007]. The formalism of Anttila et al. [2006] treats organic aerosol by regarding the organic fraction as a coating. Since it requires detailed knowledge of the aerosol mixing state, it is not compared to field data here, although the reader is referred to a recent model study (N. Riemer et al., The relative importance of organic coatings for the heterogeneous hydrolysis of N₂O₅, submitted to Journal of Geophysical Research, 2009). We note, however, that the AMS data for the night flights on which $\gamma(N_2O_5)$ were determined showed SOA-like aerosol (oxygenated organic fraction > 60%, with an average of approximately 80%) with size distributions consistent with internally mixed organic and inorganic aerosol, similar to the aerosol composition during daytime flights (R. Bahreini et al., Organic aerosol formation in urban and industrial plumes near Houston and Dallas, Texas, submitted to Journal of Geophysical Research, 2009).

[25] A second potential reason for the smaller observed $\gamma(N_2O_5)$ is the nitrate effect. Laboratory studies show that $\gamma(N_2O_5)$ is significantly smaller on pure nitrate salts (e.g., NaNO₃) than on other inorganic aerosol such as sulfate

[Hallquist et al., 2003; Mentel et al., 1999; Wahner et al., 1998b] at certain RH. Mechanistically, this effect is thought to arise from the solution phase reaction of NO₃⁻ with $H_2O \cdot NO_2^+$, the reverse of the ionization of N_2O_5 that leads to its solvation. Parameterizations of this effect generally assume a linear dependence on the NO₃ content of the bulk aerosol. Figure 11 shows the determined and parameterized $\gamma(N_2O_5)$ as a function of aerosol nitrate to nitrate + sulfate mass from the AMS. As in the previous comparisons, the determined values show no clear dependence on aerosol nitrate fraction in the inorganic phase. The Davis et al. [2008] parameterization has an upper limit that depends on this ratio, with additional variation due to the relative humidity dependence seen in Figure 9. The Riemer et al. [2003] parameterization was specifically intended to test the importance of the nitrate effect on formation of ozone and nitrate aerosol for conditions in Europe and incorporates only the linear dependence on nitrate fraction, with no RH or organic aerosol dependence. Although the determined $\gamma(N_2O_5)$ show no clear dependence on aerosol nitrate fraction, the nitrate effect may still be partly responsible for the observed smaller $\gamma(N_2O_5)$ if its dependence is nonlinear in NO₃. As previously noted by Davis et al. [2008], laboratory studies on mixed nitrate and sulfate aerosol are required to supplement the existing database on pure nitrate salts in order to characterize this effect more fully.

[26] Figure 12 summarizes the data in Figures 9–11 as a direct comparison of the parameterized to the determined $\gamma(N_2O_5)$. There is no clear relationship between the two, other than that the determined values are uniformly lower than the parameterizations. The low values are consistent, and appear to be applicable to the relative humidity range (25–72%) and aerosol composition (inorganic aerosol present as fully neutralized ammonium sulfate with measurable nitrate content, and organic content between 0.2 and 0.8 of total mass) encountered on night flights during TexAQS II. Similarly small values for $\gamma(N_2O_5)$ were determined on similar aerosol types in a previous aircraft campaign in the

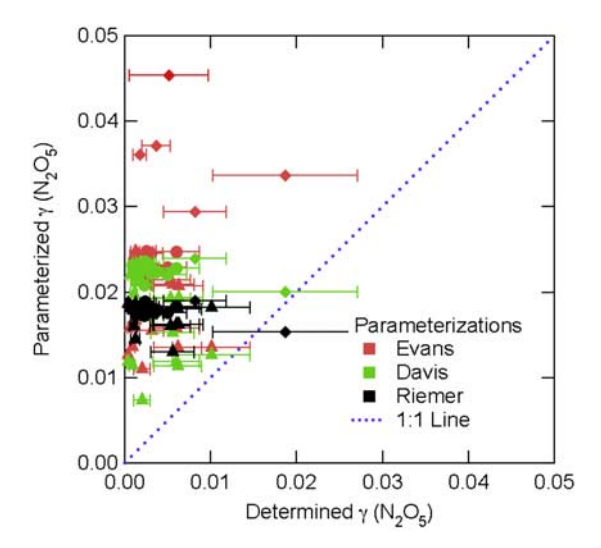


Figure 12. Direct comparison of parameterized to determined $\gamma(N_2O_5)$ to different parameterizations. The dashed line is 1:1.

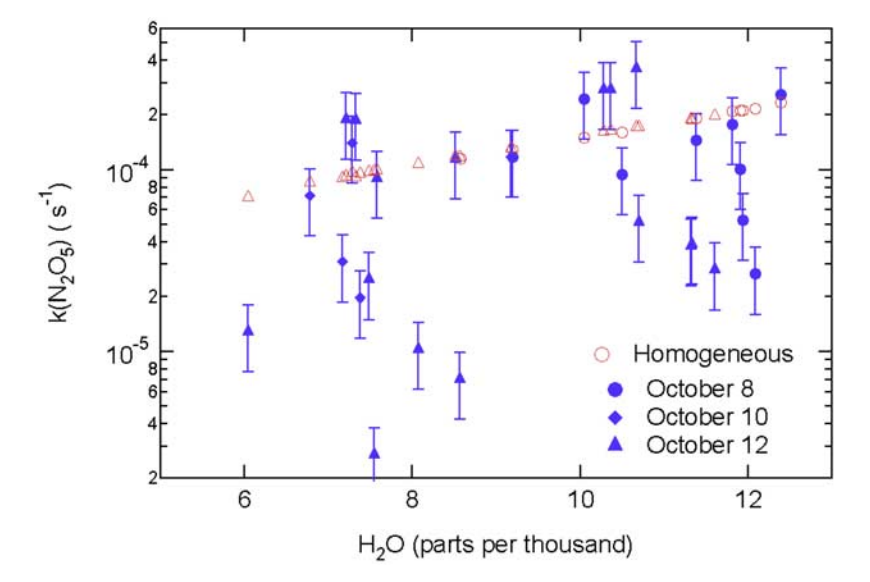


Figure 13. Plot of determined N_2O_5 first-order loss rate coefficients from fits of plume analyses to equations (5)–(7) or from plume model determinations where steady state was not applicable (see Table 2), against water vapor mixing ratio for three night flights. Also shown are predicted homogeneous hydrolysis first-order N_2O_5 rate coefficients (equation (13)) for the same time periods. Even without subtraction of heterogeneous hydrolysis, determinations are frequently smaller, and in some cases much smaller, than the homogeneous rate coefficient.

northeast United States [Brown et al., 2006b]. The lack of dependence on RH or aerosol composition in the determined values may reflect the overall uncertainty in the determinations themselves, which may be too large to elucidate such effects if they occur over a range of small $\gamma(N_2O_5)$. Our previous study identified large $\gamma(N_2O_5)$ on acidic sulfate aerosol at somewhat higher RH (65–85%) [Brown et al., 2006b]. This aerosol type was not prevalent on TexAQS II night flights.

6. Homogeneous N₂O₅ Hydrolysis

[27] The direct, gas phase reaction of N₂O₅ with water vapor provides an alternative route to hydrolysis that does not require uptake to aerosol. Mentel, Wahner and coworkers [Mentel et al., 1996; Wahner et al., 1998b] measured the first-order homogeneous hydrolysis rate coefficient in a series of chamber experiments and proposed a mechanism that was the sum of a bimolecular and a termolecular reaction with water vapor.

$$\begin{split} k_{Homo} &= k_I [H_2 O] + k_{II} [H_2 O]^2, \\ k_I &= 2.5 \times 10^{-22} \text{ cm}^3 \text{ molecule}^{-1} \text{ s}^{-1}, \\ k_{II} &= 1.8 \times 10^{-39} \text{ cm}^6 \text{ molecule}^{-2} \text{ s}^{-1}. \end{split} \tag{13}$$

The rate coefficients in equation (13) place a limit on the N_2O_5 lifetime ranging from 1.2–4 h for the water vapor concentrations encountered in this study. As Figure 13 shows, the determinations from this study show N_2O_5 to frequently have been longer lived than this limit. Figure 13 shows the first-order rate coefficients for N_2O_5 loss for the three TexAQS II night flights determined directly from fits to equations (5)–(7) or from plume modeling where the steady state approximation was not applicable. Figure 13

also shows the first-order rate coefficients from equation (13) for the same data. The determined $k_{\rm N2O5}$ are in many cases smaller than the homogeneous hydrolysis recommendation, and in some cases they are as much as a factor of 10 smaller. The determined rate coefficients, as plotted in Figure 13, do not account for heterogeneous hydrolysis. Subtraction of the heterogeneous uptake rate coefficient, if such a subtraction were possible with certainty, would lead to even smaller limits for the homogeneous hydrolysis loss rate coefficient. In any case, the comparison suggests a much smaller rate of homogeneous hydrolysis than equation (13) for use in atmospheric models. This conclusion is consistent with previous analysis from similar aircraft and ship-based measurements [Aldener et al., 2006; Brown et al., 2006b; Sommariva et al., 2008].

7. Nocturnal Halogen Activation

[28] The discussion of heterogeneous N_2O_5 uptake to this point has considered HNO₃ to be the principal reaction product (reaction (4)). Recent field [Osthoff et al., 2008] and laboratory [Behnke et al., 1997; Finlayson-Pitts et al., 1989; Thornton and Abbatt, 2005; J. M. Roberts et al., Production of ClNO₂ and Cl₂ from N_2O_5 uptake on model aerosol substrates, manuscript in preparation, 2009] studies have demonstrated that uptake to chloride-containing aerosol results in production of both HNO₃ (or aerosol phase NO_3) and nitryl chloride, ClNO₂, as follows.

$$N_2O_5(g) + Cl^-(aq) \rightarrow ClNO_2(g) + NO_3^-(aq).$$
 (14)

Nitryl chloride is stable at night but photolyzes readily in the morning to yield NO₂ and atomic chlorine, such that reaction (14) is a potentially large active halogen source in regionally polluted areas. The magnitude of this source

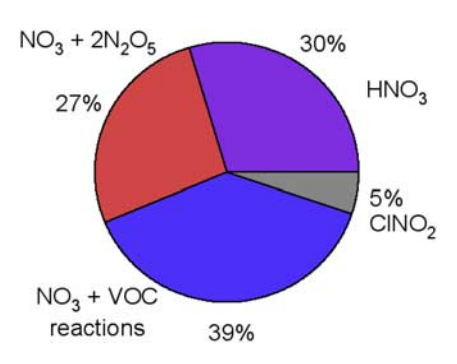


Figure 14. Pie chart showing the proportion of ClNO₂ relative to other products of nighttime NO₂ oxidation for the plume shown in Figure 8. The ClNO₂ is a calculated upper limit based on the maximum possible chloride content of the sampled aerosol.

depends upon the production rate of N_2O_5 (related to the availability of NO_x), its uptake coefficient, and the branching between reaction (14) and the conventional hydrolysis in reaction (4). Surface level measurements of $CINO_2$ during TexAQS II from a ship platform (the NOAA R/V Brown) provided the first atmospheric detection of this compound and showed surprisingly large levels (up to 1.2 ppbv) and efficient production [Osthoff et al., 2008]. Observed $CINO_2$ levels required production from N_2O_5 uptake to submicron aerosol, where the median chloride concentration was $[CI^-] = 0.05$ M.

[29] Aircraft measurements of ClNO₂ were not available during TexAQS II. Aerosol chloride measurements were also limited. The AMS measured nonrefractory aerosol chloride, but there were only brief episodes during which the Cl⁻ was present above the AMS detection limit of $0.05~\mu g~m^{-3}$, none coinciding with nocturnal NO_x plumes. The AMS limit for aerosol chloride mass and the measured aerosol volume provides an upper limit to aerosol chloride concentration if all chloride were nonrefractory (i.e., not present as sodium chloride). The corresponding upper limit to the ClNO₂ yield, defined as the amount of ClNO₂ produced per N₂O₅ taken up, can be calculated from available laboratory data [Behnke et al., 1997; Roberts et al., manuscript in preparation, 2009].

$$\Phi(ClNO_2) = \frac{ClNO_2}{\Delta N_2 O_5} = \left(\frac{k_{H2O}[H_2O]}{k_{Cl}[Cl^-]} + 1\right)^{-1}.$$
 (15)

The rate coefficients, $k_{\rm H2O}$ and $k_{\rm Cl}$ in equation (15) are for solution phase reaction of NO₂⁺ with H₂O and Cl⁻, respectively. Behnke et al. [1997] and Roberts et al. (manuscript in preparation, 2009) give the ratio $k_{\rm Cl}/k_{\rm H2O}$ = 836 and 450, respectively. Upper limits for nonrefractory aerosol chloride concentration on night flights were [Cl⁻] \leq 0.05 M – 1 M, corresponding to upper limits of $\Phi({\rm ClNO}_2) \leq$ 0.3–0.9. These limits could be larger if sodium chloride were present in the submicron aerosol. Therefore, ClNO₂ production could have been a substantial component of N₂O₅ uptake on TexAQS II night flights. The foregoing discussion has shown that although heterogeneous uptake of N₂O₅ was generally slow, it was nonzero and lead to measurable HNO₃ production, particularly for plumes with

high aerosol surface areas. The 8 October plume shown in Figure 3 can again be used as one example since nighttime HNO₃ production in this plume was among the largest observed. The limit to $\Phi(\text{ClNO}_2)$ in this plume was 0.3. Competition between reactions (4) and (14) leads to production of ClNO_2 and HNO_3 in a well-defined ratio.

$$\frac{ClNO_2}{HNO_3} = \frac{\Phi(ClNO_2)}{2 - \Phi(ClNO_2)}.$$
 (16)

The observed HNO $_3$ enhancement of 1.9 ppbv in this plume corresponds to an upper limit for ClNO $_2$ production of \leq 0.33 ppbv. Figure 14 shows the partitioning among NO $_2$ oxidation products for this plume for estimated limiting ClNO $_2$ production. If these nighttime plumes were to produce ClNO $_2$ levels comparable to these calculated limits, it would represent a significant halogen input from overnight heterogeneous chemistry. Further aircraft measurements that include both ClNO $_2$ and higher sensitivity aerosol chloride measurements will clearly be of considerable future interest.

8. Summary and Conclusions

[30] Values for heterogeneous uptake coefficients of N_2O_5 to aerosol, $\gamma(N_2O_5)$, have been determined from aircraft measurements of O₃, NO₂, NO₃, N₂O₅, and aerosol surface area. Analysis of the NO2 scaling of the steady state lifetimes of NO₃ and N₂O₅ allowed for separation of NO₃-VOC reactions from N₂O₅ uptake to aerosol. Modeling of observed HNO3 enhancements within plumes with welldefined nighttime transport times corroborated the steady state analysis. Determined $\gamma(N_2O_5)$ were low, generally smaller than 0.01 over a range of relative humidity and aerosol composition, with no clear dependence on either parameter. Aerosol sampled in Texas was primarily neutralized ammonium sulfate with a large organic fraction (>50% of total mass). By contrast, our previous aircraft measurements in the northeast United States showed a large regional variability in the distribution of sulfate aerosol and a larger variation in $\gamma(N_2O_5)$. The TexAQS II analysis further demonstrated that the current recommended rate coefficient for homogeneous N₂O₅ hydrolysis is likely too large, possibly by as much as an order of magnitude. Aerosol chloride was below the AMS detection limit and ClNO₂ was not measured from the aircraft during TexAQS II. Upper limits for ClNO₂ production based on maximum possible aerosol chloride content nevertheless allow for potentially significant nocturnal halogen activation.

[31] The determined $\gamma(N_2O_5)$ were significantly smaller than values calculated from several parameterizations used in atmospheric models. Further detailed laboratory work to define the uptake coefficients of N_2O_5 to mixed organic, sulfate, nitrate and chloride aerosol, and their relative humidity and temperature dependence, are needed for improvement of the parameterizations. Laboratory work to reexamine the rate coefficient for homogeneous reaction of N_2O_5 with water vapor may also be of interest for comparison with these field data. Further field measurements of N_2O_5 reactivity, including aircraft measurements of different reaction products such as HNO_3 and $CINO_2$, will also be of considerable future interest.

[32] **Acknowledgments.** This work was supported by the NOAA Atmospheric Chemistry and Climate Program and the Texas Air Quality Study. The authors thank Prakash Bhave for useful discussions regarding uptake coefficient parameterizations. The authors also thank the crew of the NOAA P-3 for their dedication and professionalism.

References

- Aldener, M., et al. (2006), Reactivity and loss mechanisms of NO_3 and N_2O_5 in a marine environment: Results from in situ measurements during NEAQS 2002, *J. Geophys. Res.*, 111, D23S73, doi:10.1029/2006JD007252.
- Allan, B. J., N. Carslaw, H. Coe, R. A. Burgess, and J. M. C. Plane (1999), Observations of the nitrate radical in the marine boundary layer, *J. Atmos. Chem.*, 33, 129–154, doi:10.1023/A:1005917203307.
- Allan, B. J., G. McFiggans, J. M. C. Plane, H. Coe, and G. G. McFadyen (2000), The nitrate radical in the remote marine boundary layer, *J. Geophys. Res.*, 105, 24,191–24,204.
- Allan, B. J., J. M. C. Plane, H. Coe, and J. Shillito (2002), Observations of NO₃ concentration profiles in the troposphere, *J. Geophys. Res.*, 107(D21), 4588, doi:10.1029/2002JD002112.
- Ambrose, J. L., H. Mao, H. R. Mayne, J. Stutz, R. Talbot, and B. C. Sive (2007), Nighttime nitrate radical chemistry at Appledore Island, Maine during the 2004 International Consortium for Atmospheric Research on Transport and Transformation, J. Geophys. Res., 112, D21302, doi:10.1029/2007JD008756.
- Anttila, T., A. Kiendler-Scharr, R. Tillmann, and T. F. Mentel (2006), On the reactive uptake of gaseous compounds by organic-coated aqueous aerosols: Theoretical analysis and applications to the heterogeneous hydrolysis of N₂O₅, *J. Phys. Chem. A*, 110, 10,435–10,443, doi.org/10.1021/ip062403c.
- Apodaca, Ř. L., D. M. Huff, and W. R. Simpson (2008), The role of ice in N₂O₅ heterogeneous hydrolysis at high latitudes, *Atmos. Chem. Phys. Discuss.*, 8, 12,595–12,624.
- Atkinson, R., and J. Arey (2003), Atmospheric degradation of volatile organic compounds, Chem. Rev., 103, 4605–4638, doi:10.1021/cr0206420.
- Atkinson, R., D. L. Baulch, R. A. Cox, J. N. Crowley, R. F. Hampson, R. G. Hynes, M. E. Jenkin, M. J. Rossi, and J. Troe (2004), Evaluated kinetic and photochemical data for atmospheric chemistry: Volume I gas phase reactions of O_x, HO_x, NO_x and SO_x species, *Atmos. Chem. Phys.*, 4, 1461–1738.
- Ayers, J. D., and W. R. Simpson (2006), Measurements of N₂O₅ near Fairbanks, Alaska, J. Geophys. Res., 111, D14309, doi:10.1029/ 2006JD007070.
- Badger, C. L., P. T. Griffiths, I. George, J. P. D. Abbatt, and R. A. Cox (2006), Reactive uptake of N₂O₅ by aerosol particles containing mixtures of humic acid and ammonium sulfate, *J. Phys. Chem. A*, 110, 6986–6994, doi:10.1021/jp0562678.
- Bahreini, R., J. L. Jimenez, J. Wang, R. C. Flagan, J. H. Seinfeld, J. T. Jayne, and D. R. Worsnop (2003), Aircraft-based aerosol size and composition measurements during ACE-Asia using an Aerodyne aerosol mass spectrometer, *J. Geophys. Res.*, 108(D23), 8645, doi:10.1029/2002JD003226.
- Baynard, T., E. R. Lovejoy, A. Pettersson, S. S. Brown, D. Lack, H. Osthoff, P. Massoli, S. Ciciora, W. P. Dube, and A. R. Ravishankara (2007), Design and application of a pulsed cavity ring-down aerosol extinction spectrometer for field measurements, *Aerosol Sci. Technol.*, 41, 447–462, doi:10.1080/02786820701222801.
- Behnke, W., C. George, V. Scheer, and C. Zetzsch (1997), Production and decay of ClNO₂, from the reaction of gaseous N₂O₅ with NaCl solution: Bulk and aerosol experiments, *J. Geophys. Res.*, 102, 3795–3804, doi:10.1029/96JD03057.
- Bell, N., D. Koch, and D. T. Shindell (2005), Impacts of chemistry-aerosol coupling on tropospheric ozone and sulfate simulations in a general circulation model, *J. Geophys. Res.*, 110, D14305, doi:10.1029/ 2004JD005538.
- Brock, C. A., et al. (2003), Particle growth in urban and industrial plumes in Texas, *J. Geophys. Res.*, 108(D3), 4111, doi:10.1029/2002JD002746.
- Brown, S. S., H. Stark, and A. R. Ravishankara (2003), Applicability of the steady state approximation to the interpretation of atmospheric observations of NO₃ and N₂O₅, *J. Geophys. Res.*, 108(D17), 4539, doi:10.1029/2003JD003407.
- Brown, S. S., et al. (2004), Nighttime removal of NO_x in the summer marine boundary layer, *Geophys. Res. Lett.*, 31, L07108, doi:10.1029/2004GL019412.
- Brown, S. S., et al. (2006a), Nocturnal odd-oxygen budget and its implications for ozone loss in the lower troposphere, *Geophys. Res. Lett.*, *33*, L08801, doi:10.1029/2006GL025900.
- Brown, S. S., et al. (2006b), Variability in nocturnal nitrogen oxide processing and its role in regional air quality, *Science*, 311, 67–70, doi:10.1126/science.1120120.

- Brown, S. S., et al. (2007), Vertical profiles in NO₃ and N₂O₅ measured from an aircraft: Results from the NOAA P-3 and surface platforms during NEAQS 2004, *J. Geophys. Res.*, 112, D22304, doi:10.1029/2007JD008883.
- Calvert, J. G., A. Lazrus, G. L. Kok, B. G. Heikes, J. G. Walega, J. Lind, and C. A. Cantrell (1985), Chemical mechanisms of acid generation in the troposphere, *Nature*, 317, 27–35, doi:10.1038/317027a0.
- Carslaw, N., J. M. C. Plane, H. Coe, and E. Cuevas (1997), Observations of the nitrate radical in the free troposphere at Izana de Tenerife, *J. Geophys. Res.*, 102, 10,613–10,622, doi:10.1029/96JD03512.
- Cosman, L. M., and A. K. Bertram (2008), Reactive uptake of N₂O₅ on aqueous H₂SO₄ solutions coated with 1-component and 2-component monolayers, *J. Phys. Chem. A*, 112, 4625–4635, doi:10.1021/jp8005469.
- Cosman, L. M., D. A. Knopf, and A. K. Bertram (2008), N₂O₅ reactive uptake on aqueous sulfuric acid solutions coated with branched and straight-chain insoluble organic surfactants, *J. Phys. Chem. A*, 112, 2386–2396, doi:10.1021/jp710685r.
- Davis, J. M., P. M. Bhave, and K. M. Foley (2008), Parameterization of N₂O₅ reaction probabilities on the surface of particles containing ammonium, sulfate and nitrate, *Atmos. Chem. Phys.*, 8, 5295–5311.
- Dentener, F. J., and P. J. Crutzen (1993), Reaction of N_2O_5 on tropospheric aerosols: Impact on the global distributions of NO_x , O_3 , and OH, *J. Geophys. Res.*, 98, 7149–7163, doi:10.1029/92JD02979.
- Dubé, W. P., S. S. Brown, H. D. Osthoff, M. R. Nunley, S. J. Ciciora, M. W. Paris, R. J. McLaughlin, and A. R. Ravishankara (2006), Aircraft instrument for simultaneous, in-situ measurements of NO₃ and N₂O₅ via cavity ring-down spectroscopy, *Rev. Sci. Instrum.*, 77, 034101, doi:10.1063/1.2176058.
- Evans, M. J., and D. J. Jacob (2005), Impact of new laboratory studies of N_2O_5 hydrolysis on global model budgets of tropospheric nitrogen oxides, ozone and OH, *Geophys. Res. Lett.*, 32, L09813, doi:10.1029/2005GL022469.
- Feng, Y., and J. E. Penner (2007), Global modeling of nitrate and ammonium: Interaction of aerosols and tropospheric chemistry, *J. Geophys. Res.*, 112, D01304, doi:10.1029/2005JD006404.
- Finlayson-Pitts, B. J., M. J. Ezell, and J. N. J. Pitts (1989), Formation of chemically active chlorine compounds by reactions of atmospheric NaCl particles with gaseous N₂O₅ and ClONO₂, *Nature*, 337, 241–244, doi:10.1038/337241a0.
- Folkers, M., T. F. Mentel, and A. Wahner (2003), Influence of an organic coating on the reactivity of aqueous aerosols probed by the heterogeneous hydrolysis of N_2O_5 , *Geophys. Res. Lett.*, 30(12), 1644, doi:10.1029/2003GL017168.
- Frost, G. J., et al. (2006), Effects of changing power plant NO_x emissions on ozone in the eastern United States: Proof of concept, *J. Geophys. Res.*, 111, D12306, doi:10.1029/2005JD006354.
- Fuchs, N. A., and A. G. Stugnin (1970), Highly Dispersed Aerosols, Ann Arbor Sci., Ann Arbor, Mich.
- Fuchs, H., W. P. Dubé, S. J. Ciciora, and S. S. Brown (2008), Determination of inlet transmission and conversion efficiencies for in situ measurements of the nocturnal nitrogen oxides, NO₃, N₂O₅ and NO₂, via pulsed cavity ring-down spectroscopy, *Anal. Chem.*, 80, 6010–6017, doi:10.1021/ac8007253.
- Geyer, A., and U. Platt (2002), Temperature dependence of the NO₃ loss frequency: A new indicator for the contribution of NO₃ to the oxidation of monoterpenes and NO_x removal in the atmosphere, *J. Geophys. Res.*, 107(D20), 4431, doi:10.1029/2001JD001215.
- Geyer, A., R. Ackermann, R. Dubois, B. Lohrmann, R. Müller, and U. Platt (2001), Long-term observation of nitrate radicals in the continental boundary layer near Berlin, *Atmos. Environ.*, *35*, 3619–3631, doi:10.1016/S1352-2310(00)00549-5.
- Hallquist, M., D. J. Stewart, S. K. Stephenson, and R. A. Cox (2003), Hydrolysis of N₂O₅ on sub-micron sulfate aerosols, *Phys. Chem. Chem. Phys.*, 5, 3453–3463, doi:10.1039/b301827j.
- Heintz, F., U. Platt, J. Flentje, and R. Dubois (1996), Long-term observation of nitrate radicals at the Tor Station, Kap Arkona (Rügen), *J. Geophys. Res.*, 101, 22,891–22,910, doi:10.1029/96JD01549.
- Hjorth, J., G. Ottobrini, F. Cappelani, and G. Restelli (1987), A Fourier transform infrared study of the rate constant of the homogeneous gasphase reaction of N₂O₅ + H₂O and determination of absolute infrared band intensities of N₂O₅ and HNO₃, *J. Phys. Chem.*, *91*, 1565–1568, doi:10.1021/j100290a055.
- Jones, C. L., and J. H. Seinfeld (1983), The oxidation of NO₂ to nitrate: Day and night, *Atmos. Environ.*, 17, 2370–2373, doi:10.1016/0004-6981 (83)90239-1.
- Kane, S. M., F. Caloz, and M.-T. Leu (2001), Heterogeneous uptake of gaseous N₂O₅ by (NH₄)₂SO₄, NH₄SO₄, and H₂SO₄ aerosols, *J. Phys. Chem. A*, 105, 6465–6470.
- Lamarque, J.-F., J. T. Kiehl, P. G. Hess, W. D. Collins, L. K. Emmons, P. Ginoux, C. Luo, and X. X. Tie (2005), Response of a coupled chemistry-

- climate model to changes in aerosol emissions: Global impact on the hydrological cycle and the tropospheric burdens of OH, ozone and NO_x , *Geophys. Res. Lett.*, 32, L16809, doi:10.1029/2005GL023419.
- Liao, H., and J. H. Seinfeld (2005), Global impacts of gas-phase chemistryaerosol interactions on direct radiative forcing by anthropogenic aerosols and ozone, J. Geophys. Res., 110, D18208, doi:10.1029/2005JD005907.
- Martinez, M., D. Perner, E.-M. Hackenthal, S. Külzer, and L. Schültz (2000), NO₃ at Helgoland during the NORDEX campaign in October 1996, *J. Geophys. Res.*, 105, 22,685–22,695, doi:10.1029/2000JD900255.
- Mathur, R., S. Yu, D. Kang, and K. L. Schere (2008), Assessment of the wintertime performance of developmental particulate matter forecasts with the Eta-Community Multiscale Air Quality modeling system, *J. Geophys. Res.*, 113, D02303, doi:10.1029/2007JD008580.
- McNeill, V. F., J. Patterson, G. M. Wolfe, and J. A. Thornton (2006), The effect of varying levels of surfactant on the reactive uptake of N₂O₅ to aqueous aerosol, *Atmos. Chem. Phys.*, 6, 1635–1644.
- Mentel, T. F., D. Bleilebens, and A. Wahner (1996), A study of nighttime nitrogen oxide oxidation in a large reaction chamber—The fate of NO₂, N₂O₅, HNO₃, and O₃ at different humidities, *Atmos. Environ.*, *30*, 4007–4020, doi:10.1016/1352-2310(96)00117-3.
- Mentel, T. F., M. Sohn, and A. Wahner (1999), Nitrate effect in the heterogeneous hydrolysis of dinitrogen pentoxide on aqueous aerosols, *Phys. Chem. Chem. Phys.*, 1, 5451–5457, doi:10.1039/a905338g.
- Mozurkewich, M., and J. G. Calvert (1988), Reaction Probability of N₂O₅ on aqueous aerosols, *J. Geophys. Res.*, *93*, 15,889–15,896, doi:10.1029/JD093iD12p15889.
- Neuman, J. A., et al. (2002), Fast-response airborne in situ measurements of HNO₃ during the Texas 200 Air Quality Study, *J. Geophys. Res.*, 107(D20), 4436, doi:10.1029/2001JD001437.
- Osthoff, H. D., et al. (2008), High levels of nitryl chloride in the polluted subtropical marine boundary layer, *Nat. Geosci.*, 1, 324–328, doi:10.1038/ngeo177.
- Park, S. C., D. K. Burden, and G. M. Nathanson (2007), The inhibition of N₂O₅ hydrolysis in sulfuric acid by 1-butanol and 1-hexanol surfactant coatings, *J. Phys. Chem. A*, 111, 2921–2929, doi:10.1021/jp068228h.
- Parrish, D. D., et al. (2009), Overview of the Second Texas Air Quality Study (TexAQS II) and the Gulf of Mexico Atmospheric Composition and Climate Study (GoMACCS), J. Geophys. Res., doi:10.1029/ 2009JD011842, in press.
- Pilling, M. J., and P. W. Seakins (1995), Reaction Kinetics, Oxford Univ. Press, Oxford, U. K.
- Platt, U. F., A. M. Winer, H. W. Bierman, R. Atkinson, and J. N. Pitts Jr. (1984), Measurement of nitrate radical concentrations in continental air, *Environ. Sci. Technol.*, 18, 365–369, doi:10.1021/es00123a015.
- Riemer, N., H. Vogel, B. Vogel, B. Schell, I. Ackerman, C. Kessler, and H. Hass (2003), Impact of the heterogeneous hydrolysis of N₂O₅ on chemistry and nitrate aerosol formation in the lower troposphere under photosmog conditions, *J. Geophys. Res.*, 108(D4), 4144, doi:10.1029/2002JD002436.
- Ryerson, T. B., L. G. Huey, K. Knapp, J. A. Neuman, D. D. Parrish, D. T. Sueper, and F. C. Fehsenfeld (1999), Design and initial characterization of an inlet for gas-phase NO_y measurements from aircraft, *J. Geophys. Res.*, 104, 5483–5492, doi:10.1029/1998JD100087.
- Ryerson, T. B., E. J. Williams, and F. C. Fehsenfeld (2000), An efficient photolysis system for fast response NO₂ measurements, *J. Geophys. Res.*, 105, 26,447–26,461, doi:10.1029/2000JD900389.
- Schaap, M., M. van Loon, H. M. ten Brink, F. J. Dentener, and P. J. H. Builtjes (2004), Secondary inorganic aerosol simulations for Europe with special attention to nitrate, *Atmos. Chem. Phys.*, 4, 857–874.
- Schauffler, S. M., E. Atlas, D. R. Blake, F. Flocke, R. A. Lueb, J. M. Lee-Taylor, V. Stroud, and W. Travnicek (1999), Distributions of brominated organic compounds in the troposphere and lower stratosphere, *J. Geophys. Res.*, 104, 21,513–21,536, doi:10.1029/1999JD900197.

- Smith, N., J. M. C. Plane, C.-F. Nien, and P. A. Solomon (1995), Nighttime radical chemistry in the San Joaquin valley, *Atmos. Environ.*, 29, 2887–2897, doi:10.1016/1352-2310(95)00032-T.
- Sommariva, R., et al. (2008), Radicals in the marine boundary layer during NEAQS 2004: A model study of day-time and night-time sources and sinks, *Atmos. Chem. Phys. Discuss.*, 8, 16,643–16,692.
- Stutz, J., B. Alicke, R. Ackermann, A. Geyer, A. B. White, and E. Williams (2004), Vertical profiles of NO₃, N2O₂, O₃, and NO_x in the nocturnal boundary layer: 1. Observations during the Texas Air Quality Study 2000, *J. Geophys. Res.*, 109, D12306, doi:10.1029/2003JD004209.
- Thornton, J. A., and J. P. D. Abbatt (2005), N₂O₅ reaction on submicron sea salt aerosol: Kinetics, products, and the effect of surface active organics, *J. Phys. Chem.*, 109, 10,004–10,012, doi:10.1021/jp054183t.
- Thornton, J. A., C. F. Braban, and J. P. Abbatt (2003), N₂O₅ hydrolysis on sub-micron organic aerosols: The effect of relative humidity, particle phase, and particle size, *Phys. Chem. Chem. Phys.*, *5*, 4593–4603, doi:10.1039/b307498f.
- Tie, X., G. Brasseur, L. Emmons, L. Horowitz, and D. Kinnison (2001), Effects of aerosols on tropospheric oxidants: A global model study, J. Geophys. Res., 106, 22,931–22,964, doi:10.1029/2001JD900206.
- Tie, X., et al. (2003), Effect of sulfate aerosol on tropospheric NO_x and ozone budgets: Model simulations and TOPSE evidence, *J. Geophys. Res.*, 108(D4), 8364, doi:10.1029/2001JD001508.
- Tuazon, E. C., R. Atkinson, C. N. Plum, A. M. Winer, and J. N. J. Pitts (1983), The reaction of gas phase N_2O_5 with water vapor, *Geophys. Res. Lett.*, 10, 953–956, doi:10.1029/GL010i010p00953.
- von Friedeburg, C., T. Wagner, A. Geyer, N. Kaiser, B. Vogel, H. Vogel, and U. Platt (2002), Derivation of tropospheric NO₃ profiles using off-axis differential optical absorption spectroscopy measurements during sunrise and comparison with simulations, *J. Geophys. Res.*, 107(D13), 4168, doi:10.1029/2001JD000481.
- Vrekoussis, M., N. Mihalopoulos, E. Gerasopoulos, M. Kanakidou, P. J. Crutzen, and J. Lelieveld (2007), Two-years of NO₃ radical observations in the boundary layer over the Eastern Mediterranean, *Atmos. Chem. Phys.*, 7, 315–327.
- Wahner, A., T. F. Mentel, and M. Sohn (1998a), Gas-phase reaction of N₂O₅ with water vapor: Importance of heterogeneous hydrolysis of N₂O₅ and surface desorption of HNO₃ in a large Teflon chamber, *Geophys. Res. Lett.*, 25, 2169–2172, doi:10.1029/98GL51596.
- Wahner, A., T. F. Mentel, M. Sohn, and J. Stier (1998b), Heterogeneous reaction of N_2O_5 on sodium nitrate aerosol, *J. Geophys. Res.*, 103, 31,103–31,112, doi:10.1029/1998JD100022.
- Wilson, J. C., B. G. Lafleur, H. Hilbert, W. Seebaugh, J. Fox, D. Gesler, C. A. Brock, B. J. Huebert, and J. Mullen (2004), Function and performance of a low turbulence inlet for sampling supermicron particles from aircraft platforms, *Aerosol Sci. Technol.*, 38, 790–802, doi:10.1080/027868290500841.
- Wood, E. C., T. H. Bertram, P. J. Wooldridge, and R. C. Cohen (2005), Measurements of N₂O₅, NO₂, and O₃ east of the San Francisco Bay, Atmos. Chem. Phys., 5, 483–491.
- E. Atlas, Marine and Atmospheric Chemistry, RSMAS, University of Miami, 4600 Rickenbacker Causeway, Miami, FL 33149, USA.
- R. Bahreini, C. A. Brock, S. S. Brown, W. P. Dubé, F. C. Fehsenfeld, A. M. Middlebrook, J. A. Neuman, A. R. Ravishankara, J. M. Roberts, T. B. Ryerson, and M. Trainer, Earth System Research Laboratory, NOAA, 325 Broadway, Boulder, CO 80305, USA. (steven.s.brown@noaa.gov)
- H. Fuchs, ICG-2, Forschungszentrum Jülich GmbH, D-52425 Jülich, Germany.
- H. D. Osthoff, Department of Chemistry, University of Calgary, Calgary, AB T2N 1N4, Canada.
- A. G. Wollny, Max Planck Institute for Chemistry, D-55128 Mainz, Germany.